

# Physics-based Demand Model and Fragility Functions of Industrial Tanks under Blast Loading

Flavio Stochino<sup>1\*</sup>, Fabrizio Nocera<sup>2</sup>, and Paolo Gardoni<sup>3</sup>

<sup>1</sup> Assistant Professor, Department of Civil Engineering, Environmental and Architecture, University of Cagliari, via Marengo 2, 09123 Cagliari (CA), Italy. E-mail: [fstochino@unica.it](mailto:fstochino@unica.it)

\*Corresponding author: Flavio Stochino

<sup>2</sup> PhD Student, Department of Civil and Environmental Engineering, MAE Center: Creating a Multi-Hazard Approach to Engineering, University of Illinois at Urbana-Champaign, 205 N. Mathews Ave, Urbana, IL, 61801. E-mail: [fnocera@illinois.edu](mailto:fnocera@illinois.edu)

<sup>3</sup> Professor, Department of Civil and Environmental Engineering, MAE Center: Creating a Multi-Hazard Approach to Engineering, University of Illinois at Urbana-Champaign, 205 N. Mathews Ave, Urbana, IL, 61801. E-mail: [gardoni@illinois.edu](mailto:gardoni@illinois.edu)

## Abstract

Blast hazards represent a serious threat to industrial facilities. Past explosion incidents highlight the severe consequences of such events. A probabilistic approach can help industries and designers mitigate the consequences of blast loading by better organizing industrial plants. In this paper, we propose a physics-based probabilistic demand model and formulate the reliability problem for industrial steel tanks under blast loading. Starting from a deterministic Single-Degree-of-Freedom (SDOF) model based on Donnell shallow-shell theory, we develop a correction term that improves the model accuracy due to the simplified representation of the SDOF model. We use Bayesian inference to estimate the unknown model parameters in the correction term and model error, combining predictions from the SDOF model with experimental data and any prior information. To illustrate, we estimate the reliability of an example cylindrical steel tanks subject to blast loading considering three damage levels. The reliability analysis yields a set of fragility curves that represent the conditional probability of the bending failure of the tank given a scaled distance, as the load intensity measure. Then, as an example, we use the developed fragility functions to estimate the reliability of a chemical industrial facility considering different explosion scenarios.

## Keywords

Steel tank; blast load; fragility; demand model; SDOF

Please cite this document as: Stochino, F., Nocera, F., & Gardoni, P. (2022). Physics-based Demand Model and Fragility Functions of Industrial Tanks under blast loading. Journal of Loss Prevention in the Process Industries, 77, 104798. DOI: 10.1016/j.jlp.2022.104798

## 33 **1 Introduction**

34 Blast loading represents a severe threat to industrial facilities. During their service lives, the  
35 component of industrial facilities such as tanks might be subject to blast loading from malicious  
36 or accidental explosions (Antonioni et al. 2009, Misuri et al. 2020, Ding et al. 2022, Ovidi et al.  
37 2022, Tugnoli et al. 2022). Past events have shown the vulnerability of industrial tanks to blast  
38 loading (e.g., Ibitayo et al. 2004, Zio et al. 2013.) Similarly, past events have highlighted the  
39 severe consequences of blast loading in industrial facilities, which can include fatalities, economic  
40 losses, and environmental impacts due to the release of hazardous materials (e.g., Marsh et al.  
41 2016, Damle et al. 2021, Araki et al. 2021, Suarez-Paba et al. 2022). The organization of industrial  
42 facilities requires optimizing the production characteristics considering possible natural or man-  
43 made threats to key structural elements, columns (Singh et al. 2020) and beams (Stochino et al.  
44 2021), or to the vulnerable components, steel tanks, and their consequences (e.g., Salvado et al.  
45 2017, Mayorga et al. 2019, Zhou et al. 2020, Lan et al. 2022). In this context, a probabilistic  
46 approach is necessary to account for the relevant uncertainties like aleatory uncertainties in the  
47 characteristics of the threats and epistemic uncertainties due to scarcity of data typical of low  
48 probability, high consequence events (Gardoni et al. 2002, Murphy et al. 2011). Cylindrical steel  
49 tanks represent a typical storage system characterized by a slender structure prone to buckling  
50 failure under blast loading (Hansen et al. 2010, Dadashzadeh et al. 2013, Sochet et al. 2014).  
51 Cylindrical steel tanks are typically characterized by a large ratio between thickness and height,  
52 which may yield flexural buckling in case of a horizontal load orthogonal to the tank. The  
53 performance of a cylindrical steel tank subject to blast loading represents a complex nonlinear

Please cite this document as: Stochino, F., Nocera, F., & Gardoni, P. (2022). Physics-based Demand Model and Fragility Functions of Industrial Tanks under blast loading. *Journal of Loss Prevention in the Process Industries*, 77, 104798. DOI: 10.1016/j.jlp.2022.104798

54 behavior due to the characteristics of the blast loading, i.e., a high amount of energy over a short  
55 time.

56 Past research focused on experimental tests on cylindrical steel tanks under blast loading. For  
57 example, Duong et al. (2012a,b) presented an experimental and analytical analysis of the dynamic  
58 response of a cylindrical shell under blast load while studying both the blast pressure and the  
59 structural behavior. Jiang et al. (2020) studied the structural behavior of monolithic steel tanks  
60 and polyurea-coated tanks under real field blast loading. Chen et al. (2016) analyzed full-scale  
61 validation tests of far-field air blast loading acting on deformable steel cylinders.

62 Similarly, modeling the response of cylindrical steel tanks subject to blast loading has also  
63 received much attention. Mathematical representations like differential equations can rigorously  
64 represent cylindrical steel tanks under blast loading (Donnell 1934). Similarly, the increasing  
65 computational capabilities and advances in numerical techniques have also enabled the modeling  
66 of the response of cylindrical steel tanks subject to blast loading using high-fidelity computational  
67 models of structural dynamics (e.g., Ameijeiras et al. 2016, Chen et al. 2016).

68 However, such approaches have several limitations in their use in the reliability analysis of  
69 cylindrical steel tanks subject to blast loading. For example, mathematical representations like  
70 differential equations pose a significant computational challenge when incorporating the  
71 uncertainties in the response of cylindrical steel tanks under blast loading. Similarly, high-fidelity  
72 models present a high computational cost, limiting their use in the reliability analysis with small  
73 failure probabilities.

74 Alternatively, available approaches (e.g., Duong et al. 2021a,b), including current blast design  
75 guidelines (e.g., PDC-TR 06-08), model the response of cylindrical steel tanks under blast loading

Please cite this document as: Stochino, F., Nocera, F., & Gardoni, P. (2022). Physics-based Demand Model and Fragility Functions of Industrial Tanks under blast loading. *Journal of Loss Prevention in the Process Industries*, 77, 104798. DOI: 10.1016/j.jlp.2022.104798

76 using a generalized single-degree-of-freedom (SDOF). The use of a generalized SDOF in  
77 reliability analysis based on sampling methods such as the Monte Carlo (MC) simulation to  
78 estimate the failure probabilities (Ditlevsen and Madsen 1996, Gardoni 2017). However, sampling  
79 methods are generally computationally expensive. Lastly, the developed models are structure-  
80 specific; thus, the developed models for a specific cylindrical steel tank cannot generally be used  
81 for other tanks.

82 This paper proposes a physics-based probabilistic demand model and formulates the reliability  
83 problem for cylindrical steel tanks under blast loading. In this paper, we refer to *risk* as a metric  
84 that captures the probability of occurrence and the associated consequences of a set of hazardous  
85 scenarios (Bedford and Cooke, 2001), as well as the source or cause of the hazardous scenarios  
86 (Gardoni and Murphy 2014). Similarly, *vulnerability* is defined as the susceptibility to adverse  
87 impacts and propensity to limited or delayed recovery within a hazardous scenario (Wang et al.  
88 2021). Lastly, *reliability* is defined as the probability that a system remains available or functional  
89 (Gardoni 2017). The proposed physics-based probabilistic models estimate the quantities of  
90 interest as a function of state variables that define the structural system (e.g., geometric quantities  
91 and material properties.) The proposed model combines a computationally convenient  
92 representation of the governing physical laws with an analytical correction term. In this paper, we  
93 first derive a generalized SDOF model based on Donnell (1934) shallow-shell theory. Then, we  
94 develop a correction term that improves the model accuracy due to the simplified representation  
95 of the SDOF model. The proposed physics-based probabilistic model also includes a model error  
96 term that captures the remaining model's uncertainty (Gardoni et al. 2002). We use Bayesian  
97 inference to estimate the unknown model parameters in the correction term and model error,

Please cite this document as: Stochino, F., Nocera, F., & Gardoni, P. (2022). Physics-based Demand Model and Fragility Functions of Industrial Tanks under blast loading. *Journal of Loss Prevention in the Process Industries*, 77, 104798. DOI: 10.1016/j.jlp.2022.104798

98 combining predictions from the generalized SDOF system with experimental data and any prior  
99 information. Using the proposed physics-based probabilistic model, we then formulate the  
100 reliability problem of cylindrical steel tanks under blast loading. To illustrate, we conduct a  
101 reliability analysis of an example cylindrical steel tank subject to blast loading considering three  
102 possible damage states. The reliability analysis yields a set of fragility curves conditioned on the  
103 scaled distance, which defines a load intensity measure. Then, as an example, we use the  
104 developed fragility functions to estimate the reliability of an industrial facility considering  
105 different explosion scenarios.

106 Following this Introduction, the rest of the paper is organized into six sections. Section 2  
107 presents the experimental database used in the model calibration. Section 3 briefly reviews the  
108 general mathematical formulation to develop probabilistic physics-based models. Section 4  
109 presents the proposed physics-based probabilistic demand model for the cylindrical steel tanks  
110 under blast loading. Section 5 develops the physics-based fragility functions, while Section 6  
111 presents the example.

## 112 2 Experimental database

113 The experimental data used for calibrating the proposed probabilistic model are from Ameijeiras  
114 et al. (2016), Chen et al. (2016), Jiang et al. (2020), Duong et al. (2021a,b).

115 *Table 1: Range of the values of the blast load and structural variables in the database.*

Variable	Symbol	Range
Scaled distance [m/kg <sup>1/3</sup> ]	$z$	2.24-18.19
Reflected peak pressure [kPa]	$P_{ref}$	12.1-594.8
Positive phase duration [msec]	$t_d$	0.32-43.41
Steel yielding strength [MPa]	$f_{stat}$	235-305
Steel elastic modulus [MPa]	$E_s$	170-225
Tank diameter [m]	$d$	0.6-70.0
Tank height [m]	$h$	0.9-35.0
Tank thickness [mm]	$e$	1.0-35.5

116 The collected data include the dynamic response of 27 cylindrical steel tanks subject to blast  
117 loading. Table 1 summarizes the variables of interest and their range of values.

118 The number of training data required to estimate the unknown model parameters mainly  
119 depends on the number of the unknown model parameters (Stone, 1996) . Developing physics-  
120 based probability models, in general, alleviates the need for (experimental) data by incorporating  
121 knowledge in other forms like existing (deterministic) models, and rules of physics and mechanics.  
122 In addition, as more data become available, the model can also be updated using Bayesian  
123 inference (more details in Section 4).

124

Please cite this document as: Stochino, F., Nocera, F., & Gardoni, P. (2022). Physics-based Demand Model and Fragility Functions of Industrial Tanks under blast loading. Journal of Loss Prevention in the Process Industries, 77, 104798. DOI: 10.1016/j.jlp.2022.104798

### 125 3 Review of probabilistic physics-based models

126 Gardoni et al. (2002, 2003) proposed a general mathematical formulation for developing  
127 probabilistic physics-based models while accounting for the various sources of information (i.e.,  
128 from the governing rules of physics and mechanics to the data from laboratory experiments and  
129 field measurements), as well as the different sources of uncertainty. In this section, we illustrate  
130 the general mathematical formulation for developing probabilistic physics-based models, the  
131 Bayesian model calibration, and the model selection procedure.

#### 132 3.1 General formulation of the probabilistic model

133 Following Gardoni et al. (2002, 2003), we can write the generic  $q$ -dimensional multivariate  
134 probabilistic physics-based model as

$$T_k[Y_k(\mathbf{x}, \boldsymbol{\Theta}_k)] = T_k[\hat{y}_k(\mathbf{x})] + \gamma_k(\mathbf{x}, \boldsymbol{\theta}_k) + \sigma_k \varepsilon_k, \quad k = 1, \dots, l \quad (1)$$

135 where  $T_k(\cdot)$  is a transformation function;  $Y_k(\mathbf{x}, \boldsymbol{\Theta}_k)$  is the  $k^{th}$  quantity of interest (e.g., capacity or  
136 demand);  $\hat{y}_k(\mathbf{x})$  is an existing deterministic model to predict  $Y_k$  that is typically based on rules of  
137 physics and mechanics;  $\gamma_k(\mathbf{x}, \boldsymbol{\theta}_k)$  is a correction term constructed to improve the prediction of  
138  $\hat{y}_k(\mathbf{x})$  and capture any possible bias in  $\hat{y}_k(\mathbf{x})$ ;  $\mathbf{x}$  is a vector of basic variables that characterize  $Y_k$ ;  
139  $\boldsymbol{\Theta}_k = (\boldsymbol{\theta}_k, \sigma_k)$  is a vector of unknown model parameters that need to be estimated. Also, if we let  
140  $\boldsymbol{\Sigma}$  denote the covariance matrix of  $(\sigma_1 \varepsilon_1, \dots, \sigma_l \varepsilon_l)$ , the collection of all unknown model parameters  
141 can then be written as  $\boldsymbol{\Theta} = (\boldsymbol{\theta}, \boldsymbol{\Sigma})$ , where  $\boldsymbol{\theta} = (\boldsymbol{\theta}_1, \dots, \boldsymbol{\theta}_l)$ .

142 There are three main assumptions in the generic multivariate probabilistic physics-based model  
143 as written in Equation (1). The  $\sigma_k \varepsilon_k$  is assumed an (additive) model error (additivity assumption),  
144 in which  $\sigma_k$  is assumed not to depend on  $\mathbf{x}$  (homoskedasticity assumption), and  $\varepsilon_k$  is a standard  
145 normal random variable (normality assumption). The transformation  $T_k(\cdot)$  is used to

Please cite this document as: Stochino, F., Nocera, F., & Gardoni, P. (2022). Physics-based Demand Model and Fragility Functions of Industrial Tanks under blast loading. Journal of Loss Prevention in the Process Industries, 77, 104798. DOI: 10.1016/j.jlp.2022.104798

146 (approximately) satisfy these three assumptions within the range of the data used to calibrate the  
147 model. For example, Box and Cox (1964) proposed a parameterized family of suitable  
148 transformations that can guide the selection of  $T_k(\cdot)$ .

149 Following Gardoni et al. (2002, 2003), we can write the correction term as

$$\gamma_k(\mathbf{x}, \boldsymbol{\theta}_k) = \sum_{j=1}^{N_{h,k}} \theta_{k,j} h_{k,j}(\mathbf{x}), \quad k = 1, \dots, l \quad (2)$$

150 where  $h_{k,j}(\mathbf{x}), j = 1, \dots, N_{h,k}$ , are explanatory functions that are (also) partially constructed based  
151 on the rules of physics and mechanics. A distinctive feature of the physics-based probabilistic  
152 model in Equation (1) is that it takes advantage of both first principles (i.e., the governing rules of  
153 physics and mechanics) as well as empirical information. The use of statistical tools guides in  
154 tailoring the empirical portion of the model to provide the most accurate predictions. For instance,  
155 Gardoni et al. (2002) proposed a stepwise deletion process (discuss next) to construct a  
156 parsimonious, yet accurate predictive model in which  $\gamma_k(\mathbf{x}, \boldsymbol{\theta}_k)$  includes only the terms that  
157 significantly contribute to the prediction of  $Y_k$ .

### 158 3.2 Bayesian model calibration and model selection

159 After formulating the probabilistic physics-based model in Equation (1), one can use a  
160 Bayesian approach to estimate  $\boldsymbol{\Theta}$ . The Bayesian approach combines the prior information about  
161  $\boldsymbol{\Theta}$  with the objective information from the observed data. Also, the Bayesian approach can be used  
162 to update the physics-based model as new data become available (e.g., Choe et al. 2007; Gardoni  
163 et al. 2007). To calibrate the probabilistic physics-based model, one can use both real data like  
164 data from laboratory experiments (Gardoni et al. 2002, 2003; Zhong et al. 2009), and virtual data  
165 like computer simulations (Gardoni et al. 2003; Huang et al. 2010). Also, one can use an

Please cite this document as: Stochino, F., Nocera, F., & Gardoni, P. (2022). Physics-based Demand Model and Fragility Functions of Industrial Tanks under blast loading. *Journal of Loss Prevention in the Process Industries*, 77, 104798. DOI: 10.1016/j.jlp.2022.104798

166 experimental design to identify the most informative cases to test or run and reduce the statistical  
167 uncertainty (Huang et al. 2010; Tabandeh and Gardoni 2015, Tabandeh et al. 2020).

168 Using the Bayesian approach, the statistical uncertainty in the estimates of  $\Theta$  is captured  
169 through its posterior probability density function (PDF),  $f(\Theta)$ . Specifically, to estimate  $\Theta$ , we use  
170 the Bayes theorem

$$f(\Theta) = \kappa L(\Theta)p(\Theta) \quad (3)$$

171 where  $f(\Theta)$  is the posterior PDF of  $\Theta$  containing the updated state of knowledge about  $\Theta$ ;  $L(\Theta)$  is  
172 the likelihood function that captures the objective information on  $\Theta$  contained in the data;  $p(\Theta)$  is  
173 the prior distribution reflecting our state of knowledge about  $\Theta$  before collecting the data; and  $\kappa =$   
174  $[\int L(\Theta)p(\Theta)d\Theta]^{-1}$  is a normalizing constant.

175 In the most general case, the likelihood function allows including lower-bound, upper-bound,  
176 and equality data (Gardoni et al. 2002). Data can be defined as lower-bound data if the measured  
177 values are less than the actual values of the quantity of interest. Similarly, data can be defined as  
178 upper-bound data if the measured values are greater than the actual values of the quantity of  
179 interest. Finally, data are defined as equality data if the measured values are the actual values of  
180 the quantity of interest. Following Gardoni et al. (2002), we can write the general expression of  
181  $L(\Theta)$  as

$$\begin{aligned}
& L(\boldsymbol{\Theta}) \\
& \propto \prod_i \text{observation} P \left\{ \begin{aligned} & \bigcap_{\text{equality data } k} [\sigma_k \varepsilon_{ki} = r_{ki}(\boldsymbol{\theta}_k)] \quad \bigcap_{\text{lower-bound data } k} [\sigma_k \varepsilon_{ki} \\ & > r_{ki}(\boldsymbol{\theta}_k)] \quad \bigcap_{\text{upper-bound data } k} [\sigma_k \varepsilon_{ki} < r_{ki}(\boldsymbol{\theta}_k)] \end{aligned} \right\} \quad (4)
\end{aligned}$$

182 where  $r_{ki}(\boldsymbol{\theta}_k) = T_k[Y_k] - T_k[\hat{y}_k(\mathbf{x}_i)] - \gamma_k(\mathbf{x}, \boldsymbol{\theta}_k)$  is the residual of the prediction for the  $i^{th}$   
183 datum. Under the assumptions of exact measurements and statistically independent observations,  
184 we can write the likelihood function as

$$\begin{aligned}
& L(\boldsymbol{\Theta}) \\
& \propto \prod_{\text{equality data}} \left\{ \frac{1}{\sigma_k} \varphi \left[ \frac{r_{ki}(\boldsymbol{\theta}_k)}{\sigma_k} \right] \right\} \times \prod_{\text{lower-bound data}} \left\{ \Phi \left[ -\frac{r_{ki}(\boldsymbol{\theta}_k)}{\sigma_k} \right] \right\} \times \prod_{\text{upper-bound data}} \left\{ \Phi \left[ \frac{r_{ki}(\boldsymbol{\theta}_k)}{\sigma_k} \right] \right\} \quad (5)
\end{aligned}$$

185 where  $\varphi(\cdot)$  and  $\Phi(\cdot)$  denote the standard Normal probability density function and the standard  
186 Normal cumulative density function. A discussion on the use of data when measurement errors  
187 are present can be found in Gardoni et al. (2002).

188 The prior distribution  $p(\boldsymbol{\Theta})$  can incorporate any additional information to reflect the state of  
189 knowledge about  $\boldsymbol{\Theta}$  before collecting the data. When no such information is available, one should  
190 use a prior distribution that has minimal influence on  $f(\boldsymbol{\Theta})$ . Therefore, in the absence of additional  
191 information, we can use a noninformative prior distribution  $p(\boldsymbol{\Theta}) \cong p(\boldsymbol{\Sigma})$ , where  $p(\boldsymbol{\Sigma})$  can be  
192 written as (Gardoni et al. 2002)

$$p(\boldsymbol{\Sigma}) \propto |\mathbf{R}|^{-(l+1)/2} \prod_{k=1}^l \frac{1}{\sigma_k} \quad (6)$$

193 where  $\mathbf{R}$  is the correlation matrix. In the case  $l = 1$ , i.e., for a univariate physics-based  
 194 probabilistic model, Equation (6) can be simplified in  $p(\boldsymbol{\Theta}) \propto 1/\sigma$ .

195 For practical use of the developed physics-based probabilistic model, the model selection  
 196 should aim for an accurate and unbiased model that can be easily adopted in practice. Also, from  
 197 a statistical standpoint, the inclusion of insignificant terms in  $\gamma_k(\mathbf{x}, \boldsymbol{\theta}_k)$  would lead to a loss of  
 198 precision of the estimates of  $\boldsymbol{\Theta}$  due to data over-fitting. To develop a parsimonious form of  
 199  $\gamma_k(\mathbf{x}, \boldsymbol{\theta}_k)$ , Gardoni et al. (2002) proposed a stepwise deletion process that can be summarized as  
 200 follows. We start with the complete set of explanatory functions that we believe would enhance  
 201 the predictive ability of  $\hat{y}_k(\mathbf{x})$  based on rules of physics and mechanics. After calibrating the  
 202 physics-based probabilistic model, we eliminate the  $h_{k,j}(\mathbf{x})$  whose coefficient  $\theta_{k,j}$  has the largest  
 203 posterior Coefficients Of Variation (COV). At each iteration, i.e., after each elimination, we re-  
 204 calibrate the remaining  $\boldsymbol{\Theta}$ . We then repeat this process until the posterior mean of  $\sigma_k$  has not  
 205 increased by an unacceptable amount. If the posterior mean of  $\sigma_k$  increases by an unacceptable  
 206 amount, the reduction is not desirable and the model form at one iteration before is as parsimonious  
 207 as possible. After defining the final form of the physics-based probabilistic model, we can further  
 208 combine highly correlated model parameters (e.g., if  $|\rho_{\theta_{k,i}\theta_{k,j}}| \geq 0.7$ ) as

$$\hat{\theta}_{k,i} = \mu_{\theta_{k,i}} + \rho_{\theta_{k,i}\theta_{k,j}} \frac{\sigma_{\theta_{k,i}}}{\sigma_{\theta_{k,j}}} (\theta_{k,j} - \mu_{\theta_{k,j}}) \quad (7)$$

209 where  $\mu_{\theta_{k,i}}$  and  $\sigma_{\theta_{k,i}}$  are the posterior mean and standard deviation of  $\theta_{k,i}$ . As discussed in Gardoni  
 210 et al. (2002), Equation (7) provides the best linear prediction of  $\theta_{k,i}$  as a function of  $\theta_{k,j}$ .

Please cite this document as: Stochino, F., Nocera, F., & Gardoni, P. (2022). Physics-based Demand Model and Fragility Functions of Industrial Tanks under blast loading. *Journal of Loss Prevention in the Process Industries*, 77, 104798. DOI: 10.1016/j.jlp.2022.104798

## 211 4 Proposed probabilistic demand model for industrial tanks under blast loads

212 In this section, we use the general formulation in Equation (1) to develop the proposed probabilistic  
213 demand model. In the proposed probabilistic demand model, the predicted quantity is the  
214 maximum displacement due to the blast load, i.e.,  $Y_k(\mathbf{x}, \boldsymbol{\theta}_k) = \delta w_{MAX}(\mathbf{x}, \boldsymbol{\theta})$ , with  $k = 1$ . In the  
215 following, we first formulate  $\hat{\delta}w_{MAX}(\mathbf{x})$  using a semi-analytical model for the dynamic elastic  
216 buckling of cylindrical tanks. Then, we design the correction term  $\gamma(\mathbf{x}, \boldsymbol{\theta})$  and calibrate the  
217 probabilistic model with the experimental data introduced in Section 2.

### 218 4.1 Deterministic model

219 In this section, we discuss the blast loading model and the structural semi-analytical deterministic  
220 model for the dynamic elastic buckling of cylindrical tanks based on Duong et al. (2012a,b).

#### 221 4.1.1 Blast Loading Model

222 In this paper, we consider the general case of a hemispherical explosion where the effects of ground  
223 reflection and the formation of the so-called Mach stem are considered (UFC 3-340-02).  
224 Following Friedlander (1946), we can write the blast loading time history,  $q(t)$  as

$$q(t) = P_{ref} \left(1 - \frac{t}{t_d}\right) \exp\left(\frac{-2t}{t_d}\right) \quad (8)$$

225 where  $P_{ref}$  is the reflected peak pressure, and  $t_d$  is the duration of the positive phase, i.e.,  $q(t) \geq$   
226  $0, \forall t \in [0, t_d]$ . Figure 1 shows the blast loading time history in Equation (8), highlighting the  
227 values of  $P_{ref}$  and  $t_d$ .

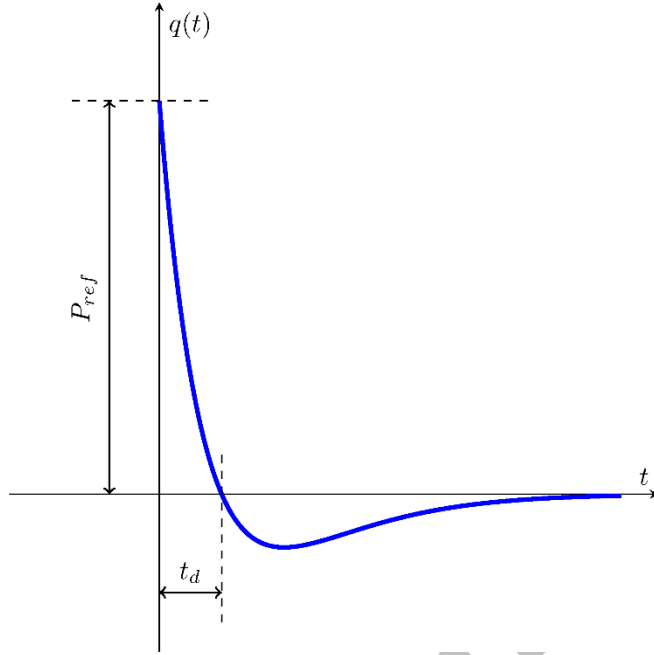


Figure 1: Blast loading time history.

228

229

230 Following Olmati et al. (2014), we can then write  $P_{ref}$  as

$$P_{ref} = 2 \cdot P_{s0} \left( \frac{7P_{atm} + 4P_{s0}}{7P_{atm} + P_{s0}} \right) \quad (9)$$

231 where  $P_{s0}$  is the stand-off pressure (expressed in MPa), and  $P_{atm}$  is the standard atmosphere  
 232 pressure, i.e.,  $P_{atm} = 0.1 \text{ MPa}$ . The stand-off pressure  $P_{s0}$  can be calculated as (Mills 1987)

$$P_{s0} = 1.772 \left( \frac{1}{z^3} \right) - 0.114 \left( \frac{1}{z^2} \right) + 0.108 \left( \frac{1}{z} \right) \quad (10)$$

233 where  $z$  is the scaled distance, i.e., the ratio between the distance from the explosive charge to the  
 234 cylindrical steel tank and the cubic root of the explosive charge. We can write the scaled distance  
 235 as

$$z = \frac{R}{W^{\frac{1}{3}}} \quad (11)$$

236 where  $R$  is the stand-off distance and  $W$  is the mass of explosives in kg of equivalent TNT (Held  
 237 1983; UFC 3-340-02.) We assume a triangular impulse, and we obtain  $t_d$  from

Please cite this document as: Stochino, F., Nocera, F., & Gardoni, P. (2022). Physics-based Demand Model and Fragility Functions of Industrial Tanks under blast loading. *Journal of Loss Prevention in the Process Industries*, 77, 104798. DOI: 10.1016/j.jlp.2022.104798

$$t_d = \frac{2 I_{s0}}{P_{s0}} \quad (12)$$

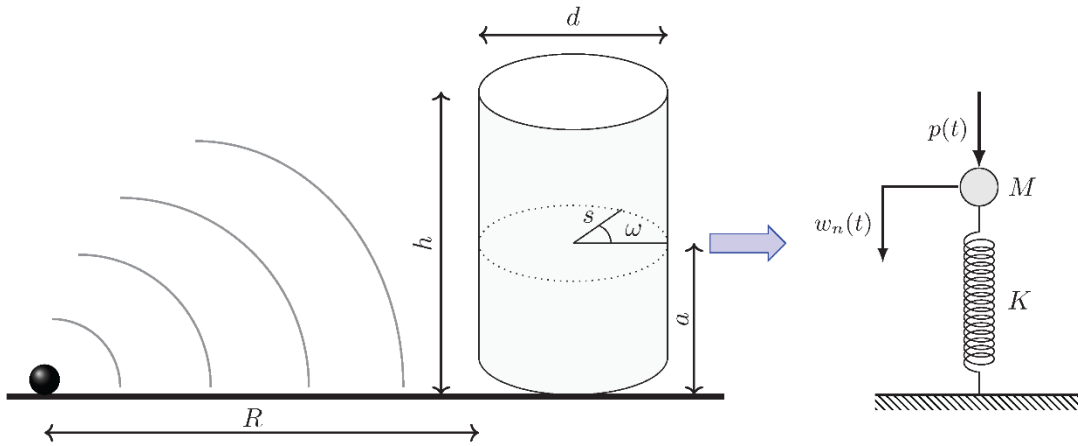
238 where  $I_{s0}$  is the incident impulse, which can be written according to Held (1983) as

$$I_{s0} = 4.8 \cdot 10^5 \cdot \frac{W^{2/3}}{R} \quad (13)$$

239 In the discussed blast loading model, we assume that the blast wave is planar and corresponds  
 240 to a uniformly distributed load on the cylindrical steel tank if the distance between the charge and  
 241 the building is sufficiently large (e.g.,  $R \geq h$ ).

#### 242 4.1.2 Structural model

243 Let us consider a cylindrical tank of height  $h$ , diameter  $d$ , and thickness  $e$ , in the cylindrical  
 244 coordinate system  $(s, \omega, a)$  as shown in Figure 2. We can express the radial displacement as  
 245  $w(s, \omega, a)$ , the axial displacement as  $u(s, \omega, a)$ , and the circumferential displacement as  
 246  $v(s, \omega, a)$ .



247  
 248 *Figure 2: Geometrical characteristics of the problem (left) and structural model (right):  $M$ ,  $K$ ,  $q$  respectively denote the*  
 249 *equivalent mass, stiffness, and load.*

250

Please cite this document as: Stochino, F., Nocera, F., & Gardoni, P. (2022). Physics-based Demand Model and Fragility Functions of Industrial Tanks under blast loading. *Journal of Loss Prevention in the Process Industries*, 77, 104798. DOI: 10.1016/j.jlp.2022.104798

251 Furthermore, based on Donnell (1934) shallow-shell theory, we enforce the Kirchhoff-Love  
 252 hypotheses with further simplifications justified by the slenderness of the cylindrical steel tanks.  
 253 It follows that  $u$  and  $v$  are negligible compared to  $w$ , the curvature variations and the partial  
 254 derivatives of  $w$  are small, and the product of the partial derivatives of  $w$  have the same order of  
 255 magnitude of strains.

256 If the shell is initially in a membrane state under a lateral pressure  $q$  so that there is a distributed  
 257 circumferential stress  $N_\omega$  (while the axial and shear stress are negligible  $N_s = N_{s\omega} = 0$ ), we can  
 258 write the dynamic equilibrium equation as follows, see Duong (2012b):

$$D\nabla^4 \delta w = -\frac{2q}{d} \frac{\partial^2 \delta w}{\partial \omega^2} + \frac{2}{d} \frac{\partial^2 \delta F}{\partial s^2} - \rho e \frac{\partial^2 \delta w}{\partial t^2} \quad (14)$$

259 where  $\rho$  is the specific mass,  $F_A(s, \omega, a)$  is the Airy stress function defined in the next Equation  
 260 (15):

$$N_s = \frac{4}{d^2} \frac{\partial^2 F_A}{\partial \omega^2}, \quad N_\omega = \frac{\partial^2 F_A}{\partial s^2}, \quad N_{s\omega} = -\frac{2}{d} \frac{\partial^2 F_A}{\partial \omega \partial s} \quad (15)$$

261 where  $N_\omega$  is the circumferential stress,  $N_s$  is the axial stress and  $N_{s\omega}$  denote the shear stress,  $B$  is  
 262 a stiffness parameter equal to  $E_s e^3 / (12(1 - \nu^2))$ ,  $E_s$  is the steel elastic modulus,  $\nu$  is the Poisson  
 263 coefficient,  $e$  is the tank thickness.

264 Also, to account for the strain rate effects due to the high loading rate of blast loading, we use  
 265 a Dynamic Increase Factor  $DIF = \frac{f_{dyn}}{f_{stat}} = 1.17$ , where  $f_{dyn}$  is the dynamic yielding strength and  
 266  $f_{stat}$  is the static one (UFC 3-340-02).

267 We assume that, during buckling, the cylindrical tank will present a doubly periodic surface  
 268 expressed by the sum of  $m$  half-waves in the axial direction and  $n$  full waves in the circumferential

Please cite this document as: Stochino, F., Nocera, F., & Gardoni, P. (2022). Physics-based Demand Model and Fragility Functions of Industrial Tanks under blast loading. Journal of Loss Prevention in the Process Industries, 77, 104798. DOI: 10.1016/j.jlp.2022.104798

269 one. Thus, we write the out-of-plane displacement field  $\delta w$  and the Airy function  $\delta F$  by using the  
 270 Fourier expansion representation as

$$\delta w(s, \omega, t) = \sum_{m=1}^{\infty} \sum_{n=1}^{\infty} \delta w_{mn}(t) \sin\left(\frac{m\pi s}{h}\right) \sin(n\omega) \quad (16)$$

$$\delta F_A(s, \omega, t) = \sum_{m=1}^{\infty} \sum_{n=1}^{\infty} \delta F_{A_{mn}}(t) \sin\left(\frac{m\pi s}{h}\right) \sin(n\omega) \quad (17)$$

271 We then define  $\lambda = 2nh/\pi d$ , and using the Fourier expansion representation in Equation (14),  
 272 we can write

$$\left( \frac{B\pi^4}{h^4} (m^2 + \lambda^2)^2 + \frac{4m^4 Ee}{d^2} (m^2 + \lambda^2)^{-2} - \frac{q(t)d\pi^2}{2h^2} \lambda^2 \right) \delta w_{mn}(t) = \rho e \delta \ddot{w}_{mn}(t) \quad (18)$$

273 Following Duong et al. (2012b), we assign an initial radial shape imperfection  $\delta w_n^i$  to each mode  
 274  $n$ . Then, we study the elastic dynamic buckling based on the amplification of such imperfections.  
 275 In this paper, we use  $\delta w_n^i = 8.33 \cdot 10^{-7} \cdot h/e$  as suggested in Duong (2012b).

276 Experimental results show that  $m = 1$  and  $n \gg 1$  so that  $1 + \lambda^2 \approx \lambda^2$  and Equation (18)  
 277 becomes:

$$\left( \frac{16B\pi^4}{d^4} + \frac{Ee\pi^4 d^2}{4n^4 h^4} \right) \delta w_n(t) - \frac{2q(t)n^2}{d} (\delta w_n(t) + \delta w_n^i) = -\rho e \delta \ddot{w}_{mn}(t) \quad (19)$$

278 Equation (19) is the Equation of motion of a single degree of freedom mass-spring system (Ruiz  
 279 et al. 1989; Duong et al. 2012b), which can be written as

$$\delta w_n(t) - \frac{q(t)}{Q_n} (\delta w_n(t) + \delta w_n^i) = -\frac{\ddot{w}_{mn}(t)}{\Omega_n^2} \quad (20)$$

280 where  $Q_n = (16Bn^4/d^4 + Ee\pi^4 d^2/(4n^4 h^4))/(\rho e)$ , and  $\Omega_n = (16Bn^4/(d^4) + Ee\pi^4 d^2/$   
 281  $(4n^4 h^4))/(2n^2/d)$ .

Please cite this document as: Stochino, F., Nocera, F., & Gardoni, P. (2022). Physics-based Demand Model and Fragility Functions of Industrial Tanks under blast loading. Journal of Loss Prevention in the Process Industries, 77, 104798. DOI: 10.1016/j.jlp.2022.104798

282 We solve Equation (20) using an explicit finite difference scheme, obtaining the coefficients of the  
283 Fourier expansion defining  $\delta w(s, \omega, a)$  in Equation (16). Using this solution, we then obtain the  
284 time history of the displacements, as well as the location and the estimates of the maximum  
285 displacement  $\hat{\delta}w_{MAX}(\mathbf{x})$ .

## 286 4.2 Correction terms

287 In this section, we design  $\gamma(\mathbf{x}, \boldsymbol{\theta})$  to capture the physical characteristics not fully represented by  
288  $\hat{\delta}w_{MAX}(\mathbf{x})$ . As the candidate explanatory functions, we define  $h'_1(\mathbf{x}) = 1$  that captures the  
289 potential bias in  $\hat{\delta}w_{MAX}(\mathbf{x})$ ;  $h_2(\mathbf{x}) = z/d$ ;  $h_3(\mathbf{x}) = f_{stat}/E_s$ ;  $h_4(\mathbf{x}) = h/e$ ;  $h_5(\mathbf{x}) = h/d$ ;  
290  $h_6(\mathbf{x}) = (t_d \cdot P_{ref})/I_{SO}$ ;  $h_7(\mathbf{x}) = (d \cdot I_{SO})/(t_d \cdot e \cdot f_{stat})$ . In the proposed model, the  
291 explanatory functions are then standardized as follows

$$h_j(\mathbf{x}) = \frac{h'_j(\mathbf{x}) - \mathbb{E}[h'_j(\mathbf{x})]}{\text{Var}[h'_j(\mathbf{x})]}, j > 1 \quad (21)$$

292 Table 2 lists the minimum and maximum values, the mean, and the standard deviation of the  
293 designed explanatory functions. The proposed probabilistic model can be used for cylindrical steel  
294 tanks whose explanatory functions fall within the ranges in Table 2. However, if additional data  
295 become available, the model parameters can be updated to expand the range of applicability of the  
296 model.

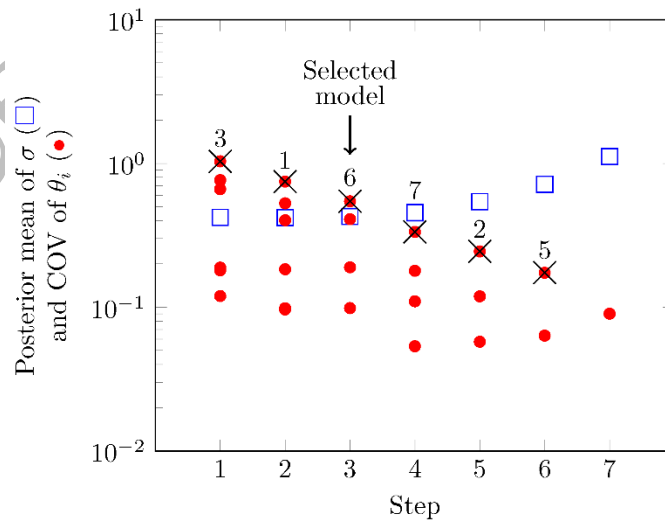
Table 2: Statistics of the designed explanatory functions.

Explanatory function	Min	Max	Mean	Standard deviation
$h'_2(\mathbf{x})$	0.04	35.95	5.83	9.16
$h'_3(\mathbf{x})$	0.00104	0.00145	0.00128	0.00016
$h'_4(\mathbf{x})$	905	2400	1121.35	463.95
$h'_5(\mathbf{x})$	0.51	4	2.10	1.32
$h'_6(\mathbf{x})$	3.52	11.44	5.49	1.80
$h'_7(\mathbf{x})$	0.005	0.94	0.18	0.25

298

299 **4.3 Bayesian model calibration and model selection**

300 In this section, we reduce the number of  $h_j(\mathbf{x})$ 's in  $\gamma(\mathbf{x}, \boldsymbol{\theta})$  using the stepwise deletion process  
 301 described in Section 3.2 to obtain a parsimonious model. Figure 4 shows the posterior COV of  
 302 the model parameters  $\boldsymbol{\theta}$  and the posterior mean of  $\sigma$  at each iteration in the stepwise deletion  
 303 process.



304

305

Figure 3: Stepwise deletion process of the proposed probabilistic model.

Please cite this document as: Stochino, F., Nocera, F., & Gardoni, P. (2022). Physics-based Demand Model and Fragility Functions of Industrial Tanks under blast loading. Journal of Loss Prevention in the Process Industries, 77, 104798. DOI: 10.1016/j.jlp.2022.104798

306 We stop the stepwise deletion process at Step 3, resulting in the final form  $\gamma(\mathbf{x}, \boldsymbol{\theta})$  as

$$\gamma(\mathbf{x}, \boldsymbol{\theta}) = \theta_2 h_2(\mathbf{x}) + \theta_4 h_4(\mathbf{x}) + \theta_5 h_5(\mathbf{x}) + \theta_7 h_7(\mathbf{x}) \quad (22)$$

307 Table 3 lists the posterior statistics of  $\boldsymbol{\theta}$ .

308 *Table 3: Posterior statistics of the proposed probabilistic model.*

Parameter	Mean	Standard deviation	Correlation coefficient					
			$\theta_2$	$\theta_4$	$\theta_5$	$\theta_7$	$\sigma$	
$\theta_2$	0.73	0.13	1					
$\theta_4$	-1.99	0.11	0.46	1				
$\theta_5$	1.29	0.14	0.59	0.45	1			
$\theta_7$	0.43	0.14	0.63	0.35	0.71	1		
$\sigma$	0.45	0.07	0.03	0.02	0.05	0.04	1	

309 Figure 5 shows a comparison between the measured and predicted values of the maximum  
310 displacements for all the cylindrical tanks in the database. In Figure 5, the left plot shows the  
311 predictions based on the deterministic model, whereas the right plot shows the predictions based  
312 on the probabilistic model. For the probabilistic model, median predictions ( $\varepsilon = 0$ ) are shown,  
313 and the dotted lines delimit the region within 1 standard deviation of the median.

314

315

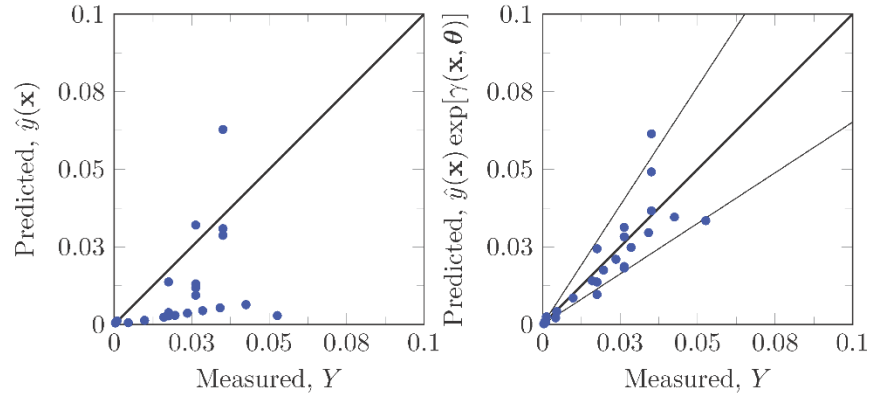


Figure 4: Comparison between measured and predicted values based on deterministic (left) and probabilistic (right) models.

316

317  
318

319

320 The deterministic model on the left is strongly biased since it underestimates the maximum  
321 displacement due to the blast load, i.e., most of the data lie below the 1:1 line. Instead, the  
322 probabilistic model on the right corrects this bias and properly accounts for all the prevailing  
323 uncertainties.

### 324 5 Fragility functions using the proposed probabilistic demand model

325 Fragility functions are defined as the conditional probability of attaining or exceeding a specified  
326 performance level given a (set of) intensity measure(s) (Gardoni et al. 2002, 2003, Nocera et al.  
327 2019). Gardoni et al. (2002, 2003) proposed to develop fragility functions by conducting a  
328 rigorous reliability analysis considering limit-state function(s) expressed in terms of the structural  
329 capacity and the corresponding imposed demands. After developing the physics-based  
330 probabilistic demand model according to Equation (1), we can write the limit-state function as  
331 (Gardoni 2017)

$$g(\mathbf{x}, \boldsymbol{\theta}) = C(\mathbf{x}) - D(\mathbf{x}, \boldsymbol{\theta}) \quad (23)$$

332 where  $C$  and  $D$  are the capacity and demand models associated with the considered failure mode.

Please cite this document as: Stochino, F., Nocera, F., & Gardoni, P. (2022). Physics-based Demand Model and Fragility Functions of Industrial Tanks under blast loading. *Journal of Loss Prevention in the Process Industries*, 77, 104798. DOI: 10.1016/j.jlp.2022.104798

333 For the capacity, performance thresholds (e.g., PDC-TR 06-08) can be defined considering the  
334 value of bending rotation  $\alpha$ , see Table 4. Alternatively, one could develop a probabilistic capacity  
335 model following the general form in Equation (1).

336 *Table 4: Bending rotation performance thresholds.*

Component Damage Level	$\alpha$ [°]
Blowout	12
Hazardous Failure	6
Heavy Damage	2

337  
338 Similarly, we translate the estimates of the maximum displacement into the corresponding bending  
339 rotation. We linearize the curvature distribution around the maximum displacement, and we  
340 estimate the bending rotation  $\alpha$  via geometrical considerations. Figure 3 shows the bending  
341 rotation scheme along the cylindrical tank perimeter and the geometrical characteristics used to  
342 estimate  $\alpha$ . In Figure 3,  $\delta w_{MAX}$  is the tank maximum radial displacement pointed by  $\omega_c$  in the  
343 cylindrical coordinate system and  $\delta w_{min}$  represents the closest minimum distance between the  
344 deformed tank and the tank center. Both  $\delta w_{MAX}$  and  $\delta w_{min}$  are obtained with the model presented  
345 in the previous sections.

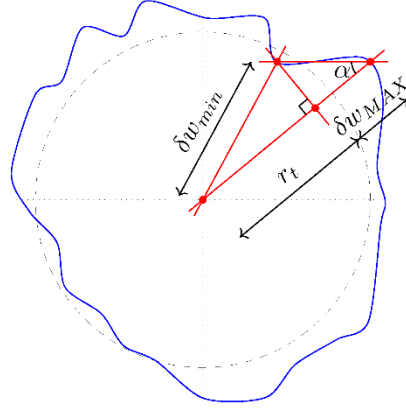


Figure 5: Bending rotation scheme along the cylindrical tank perimeter.

346

347

348

349 We can then write  $\alpha$  as

$$\alpha = \tan^{-1} \frac{(r_t - \delta w_{min}) \sin(\omega_c)}{r_t + \delta w_{MAX} - (r_t - \delta w_{min}) \cos(\omega_c)} \quad (24)$$

350 where  $r_t$  is the tank radius.

351 The proposed performance thresholds can be linked to currently applied approaches for  
 352 defining release scenarios in the case of quantitative risk analysis. As a first approximation, we  
 353 can refer to the Loss Of Containments events LOCs for stationary single-containment atmospheric  
 354 tanks (see Uijt et al. 2005, and Landucci et al. 2020). For example, the blowout threshold can be  
 355 equal to the instantaneous release of the complete inventory to the atmosphere, the Hazardous  
 356 Failure threshold can be equal to the continuous release of the complete inventory to the  
 357 atmosphere at a constant rate of release in 10 min, while the Heavy Damage threshold is equal to  
 358 the continuous release from an equivalent release diameter of 10-50 mm.

359 Next, let  $\mathbf{x} = (\mathbf{r}, z)$  where  $\mathbf{r}$  is the set of state variables that characterizes the system like  
 360 material properties, and  $z$  is the scaled distance that represent chosen intensity measure, we can  
 361 then write the fragility function as

Please cite this document as: Stochino, F., Nocera, F., & Gardoni, P. (2022). Physics-based Demand Model and Fragility Functions of Industrial Tanks under blast loading. Journal of Loss Prevention in the Process Industries, 77, 104798. DOI: 10.1016/j.jlp.2022.104798

$$F(z, \Theta) = P[g(\mathbf{x}, z, \Theta) \leq 0 | z, \Theta] \quad (25)$$

362 Depending on the treatment of uncertainty in  $\Theta$ , we can obtain two estimates of fragility  
 363 functions (Gardoni et al. 2002). The first option is to neglect the uncertainty in  $\Theta$  and use a fixed  
 364 value  $\hat{\Theta}$  (e.g., the posterior mean or mode of  $\Theta$ ) and obtain a point-estimate of the fragility  $\hat{F}(z) =$   
 365  $F(z, \hat{\Theta})$ . The second option is to account for the uncertainty in  $\Theta$  and estimate a predictive estimate  
 366 of the fragility  $\tilde{F}(z)$  as

$$\tilde{F}(z) = \int F(z, \Theta) f(\Theta) d\Theta \quad (26)$$

367 Furthermore, following Gardoni et al. (2002), we obtain confidence bounds on the estimate in  
 368 Equation (10). We can define the reliability index as

$$\beta(z, \Theta) = \Phi^{-1}[1 - F(z, \Theta)] \quad (27)$$

369 where  $\Phi^{-1}[\cdot]$  is the inverse of the standard Normal cumulative density function. The variance of  
 370  $\beta(z, \Theta)$  can then be estimated as (Gardoni et al. 2002)

$$\sigma_{\beta}^2(z) \cong \nabla_{\Theta} \beta(z) \Sigma_{\Theta\Theta} \nabla_{\Theta} \beta(z)^T \quad (28)$$

371 where  $\nabla_{\Theta} \beta(z)$  is the gradient of  $\beta(z, \Theta)$  evaluated at the mean value; and  $\Sigma_{\Theta\Theta}$  is the estimated  
 372 covariance matrix. The gradient vector  $\nabla_{\Theta} \beta(z)$  is obtained by performing a first-order reliability  
 373 method (FORM) analysis (Ditlevsen and Madsen 1996). Therefore, we can obtain bounds on  $\tilde{F}(z)$   
 374 in terms of the desired number of standard deviations away from the mean. For example, bounds  
 375 representing approximately 15% and 85% probability levels can be expressed as

$$\{\Phi[-\tilde{\beta}(z) - \sigma_{\beta}(z)], \Phi[-\tilde{\beta}(z) + \sigma_{\beta}(z)]\} \quad (29)$$

376 where  $\tilde{\beta}(z) = \Phi^{-1}[\tilde{F}(z)]$ .

377

Please cite this document as: Stochino, F., Nocera, F., & Gardoni, P. (2022). Physics-based Demand Model and Fragility Functions of Industrial Tanks under blast loading. *Journal of Loss Prevention in the Process Industries*, 77, 104798. DOI: 10.1016/j.jlp.2022.104798

378 **6 Fragility functions of an example tank and reliability of an industrial plant**

379 In this section, we develop the fragility functions of an example cylindrical steel tank subject to  
380 blast loading. A significative case study is represented by the water tanks for cooling tower systems  
381 in chemical industries. Then, we use the developed fragility functions to estimate the reliability  
382 of a typical industrial plant. Table 5 summarizes the geometry of the considered cylindrical steel  
383 tank and material properties along with their statistical information. The distance between the tank  
384 and the TNT explosive charge is 20 m to satisfy the planar blast wave hypothesis. The scaled  
385 distance  $z$  varies from 3.5 to 8 m/kg<sup>1/3</sup> by changing the mass of the TNT explosive charge.

386

Table 5: Geometry and material properties of the example tank.

Variable	Value	COV	Distribution
$d$ [m]	18	-	-
$h$ [m]	12	-	-
$e$ [mm]	5	-	-
$E_s$ [GPa]	210	-	-
$f_{yd}$ [MPa]	235	0.05	Lognormal
$\nu$	0.3	-	-
$\rho$ [kg/m <sup>3</sup> ]	7850	-	-

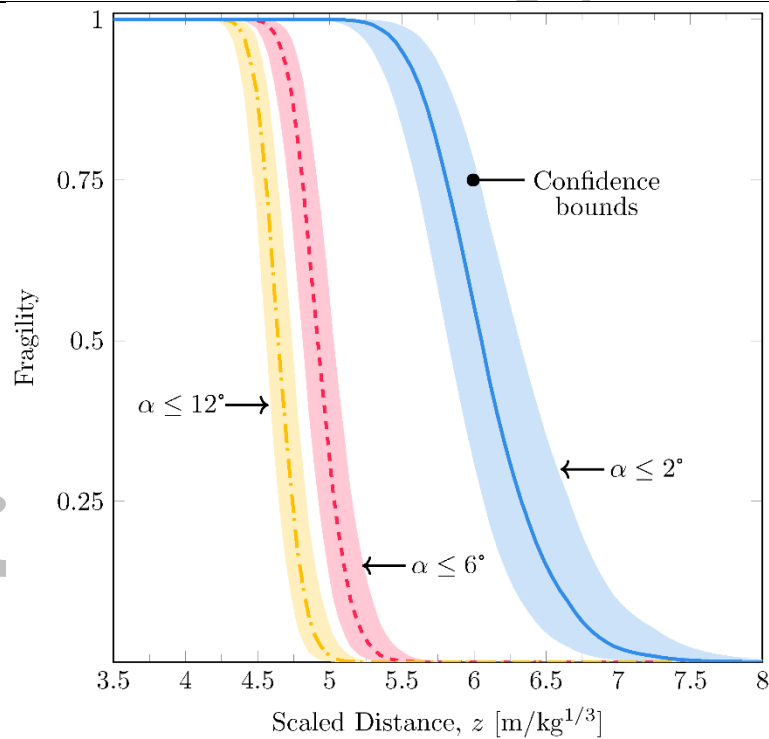


Figure 6: Fragility functions for the three capacity performance thresholds.

388

389

390 Figure 6 shows the computed fragility functions for the three capacity performance thresholds

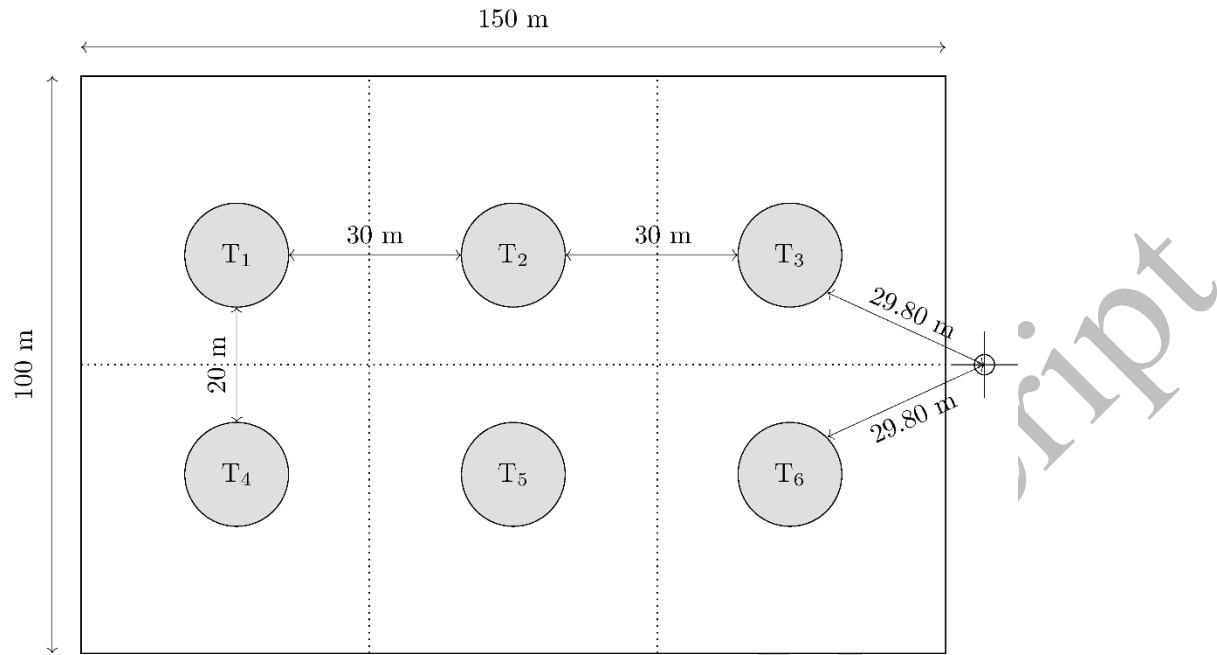
391 listed in Table 4. The solid curves in the figure represent the predictive estimate of the fragility

Please cite this document as: Stochino, F., Nocera, F., & Gardoni, P. (2022). Physics-based Demand Model and Fragility Functions of Industrial Tanks under blast loading. *Journal of Loss Prevention in the Process Industries*, 77, 104798. DOI: 10.1016/j.jlp.2022.104798

392 function  $\tilde{F}(z)$ . The shaded area around the predictive estimate represents the 15 and 85%  
393 confidence bounds due to the uncertainty in the estimate of the model parameters  $\Theta$ .

394 The computed fragility functions can be useful in the early design of a tank, in the risk analysis  
395 of an industrial plant containing the tank, or, in a more general setting, in a supply chain reliability  
396 analysis where the tank could represent one of the elements in the supply chain. To illustrate, we  
397 use the developed fragility functions to estimate the reliability of a typical industrial plant for three  
398 different threat scenarios. Figure 7 shows the layout of the example industrial plant, including the  
399 location of the tanks and their relative distances and the location of the TNT explosive charge for  
400 the three considered threat scenarios. Tables A1-A3 (in the Appendix) show the values of  $z$  for  
401 each tank. In this example, we assume the tanks contain non-inflammable material (i.e., water) so  
402 that cascading explosive charges do not occur. However, the formulation can be expanded to  
403 account for domino effects studies because (i) the formulation is developed by bringing in the  
404 physics of the problem, and (ii) the modeling is done considering state variables, which describe  
405 the dynamic state of tanks. For instance, the initial explosion of a tank may affect the state  
406 variables in the developed demand model. Specifically, shock deterioration models (e.g.,  
407 Iannacone and Gardoni 2019) can be tailored to the case of industrial steel tanks under blast loading  
408 to implement the proposed approach in a more comprehensive quantitative risk analysis  
409 framework.

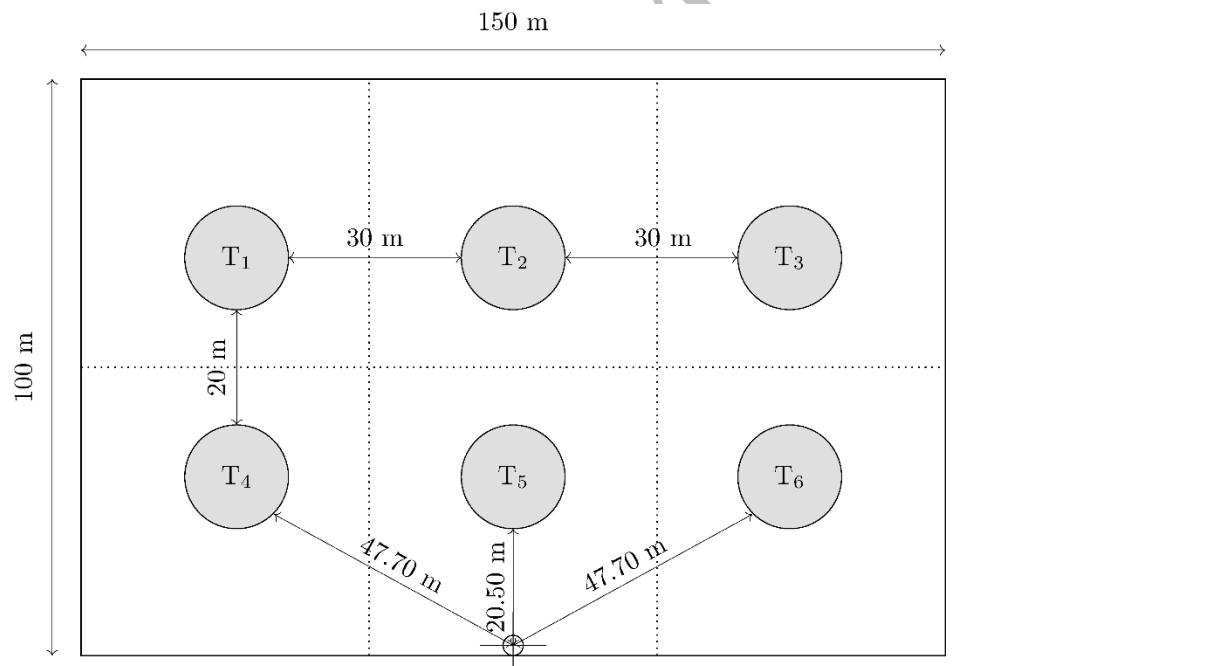
Please cite this document as: Stochino, F., Nocera, F., & Gardoni, P. (2022). Physics-based Demand Model and Fragility Functions of Industrial Tanks under blast loading. *Journal of Loss Prevention in the Process Industries*, 77, 104798. DOI: 10.1016/j.jlp.2022.104798



410

411

(a) First scenario

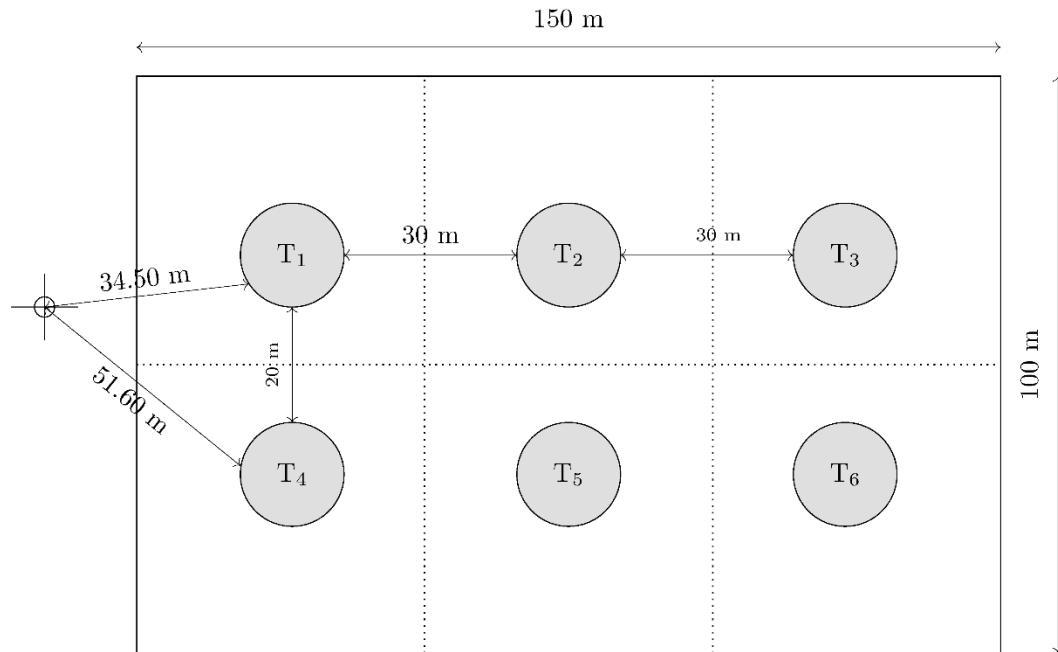


412

413

(b) Second scenario

Please cite this document as: Stochino, F., Nocera, F., & Gardoni, P. (2022). Physics-based Demand Model and Fragility Functions of Industrial Tanks under blast loading. *Journal of Loss Prevention in the Process Industries*, 77, 104798. DOI: 10.1016/j.jlp.2022.104798



(c) Third Scenario

Figure 7: Layout of the example industrial plant and location of the TNT explosive charge for the three considered scenarios.

414

415

416

417

418

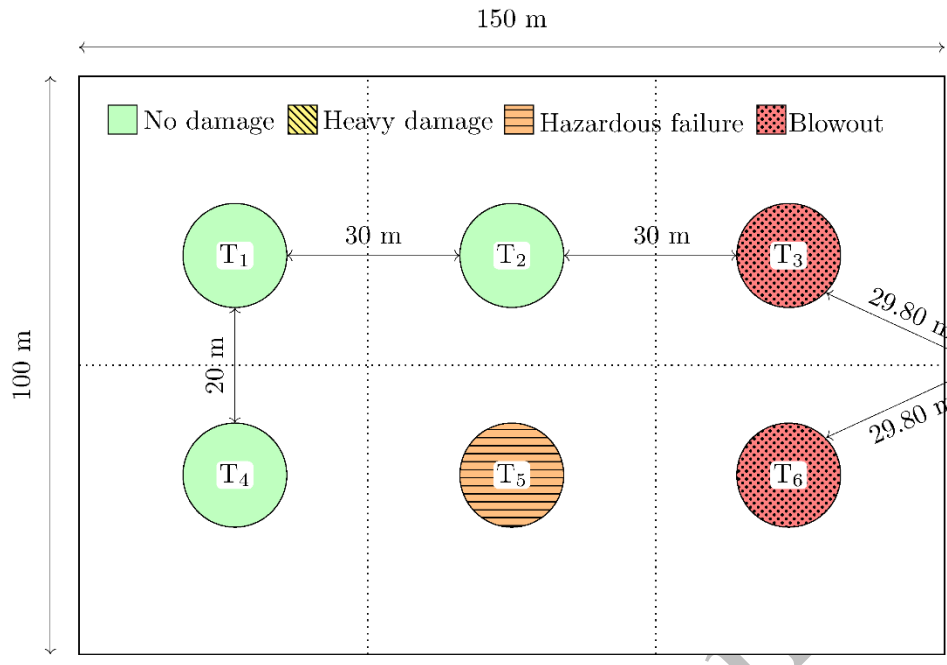
419

420

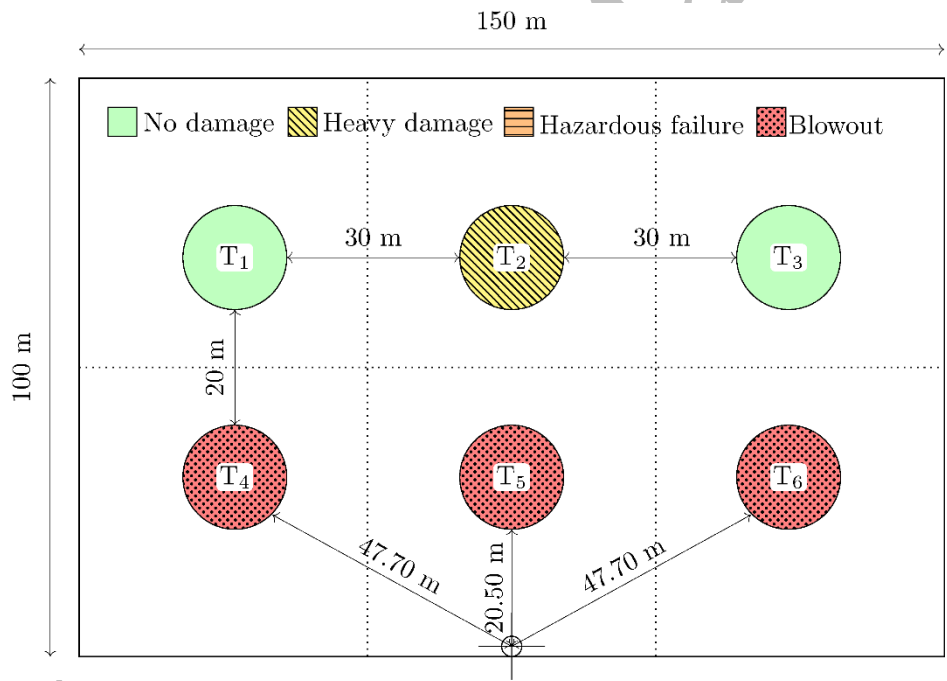
421

422

Using the fragility functions in Figure 6, we then estimate the probabilities of each tank being in each damage state based on the definition in Table 4, i.e., heavy damage, hazardous failure, and blowout. Figure 8 shows the considered tanks in the industrial plant labeled according to the most likely damage state due to the blast loading.



(a) First scenario



(b) Second scenario

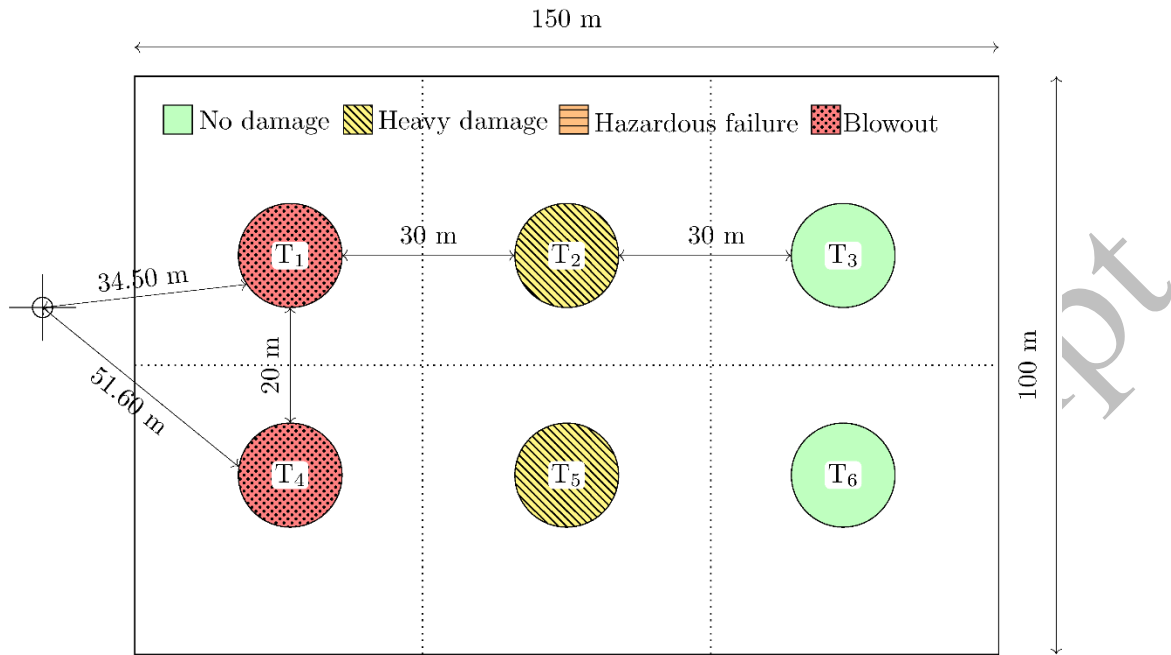
423

424

425

426

Please cite this document as: Stochino, F., Nocera, F., & Gardoni, P. (2022). Physics-based Demand Model and Fragility Functions of Industrial Tanks under blast loading. *Journal of Loss Prevention in the Process Industries*, 77, 104798. DOI: 10.1016/j.jlp.2022.104798



(c) Third scenario

Figure 8: Most likely damage state of each tank in the example industrial plant.

427  
428  
429  
430  
431  
432  
433  
434  
435  
436  
437  
438  
439  
440

In the first scenario, Tanks 1, 2 and 4 do not suffer any damage; Tanks 3 and 6 are most likely to be in the blowout damage state, whereas Tank 5 is most likely to be in the hazardous failure domain. Similarly, in the second scenario considered, Tanks 1 and 3 do not suffer any damage, whereas Tank 2 is most likely heavily damaged. All the remaining tanks are expected to be in the blowout damage state. Lastly, in the third scenario, Tanks 3 and 6 do not suffer any damage; Tanks 2 and 5 are most likely to be heavily damaged, and Tanks 1 and 4 are expected to be in the blowout damage state. In all the considered scenarios, if the scaled distance  $z$  is at least equal to 6.20 the tanks are expected not to experience any damage. Similarly, for values of  $z$  less or equal to 4.60 the tanks are expected to be in the most severe damage state.

Please cite this document as: Stochino, F., Nocera, F., & Gardoni, P. (2022). Physics-based Demand Model and Fragility Functions of Industrial Tanks under blast loading. *Journal of Loss Prevention in the Process Industries*, 77, 104798. DOI: 10.1016/j.jlp.2022.104798

441 **7 Conclusions**

442 Blast loading represents a severe threat to industrial facilities. During their service lives, the  
443 component of industrial facilities such as tanks might be subject to blast loading from malicious  
444 or accidental explosions. The paper proposed a novel probabilistic demand model for industrial  
445 steel tanks under blast loading. The proposed probabilistic demand model combines the  
446 predictions of a simplified deterministic model with an analytical correction term. We used a  
447 generalized single-degree-of-freedom (SDOF) system as the simplified deterministic model based  
448 on shallow-shell theory. Then, we developed an analytical correction term that captures the  
449 physical characteristics not fully represented by the deterministic model. The model also included  
450 an error term that captures unexplained uncertainty. We used Bayesian inference to estimate the  
451 unknown model parameters in the correction and the error terms from experimental data found in  
452 literature. Then, we used the proposed demand model to estimate the fragility functions of a typical  
453 cylindrical steel tank. The computed fragility functions can be useful in the early design of a tank,  
454 in the risk analysis of an industrial plant containing the tank, or, in a more general setting, in a  
455 supply chain reliability analysis where the tank could represent one of the components in the  
456 supply chain. To illustrate, we used the derived fragility functions to estimate the reliability of a  
457 typical industrial plant under three different malicious explosion scenarios.

458 Further developments of this research are expected considering the cascading effects of the damage  
459 to the tanks on the performance of industrial facilities at the plant level and the supply chain.

460

461 **References**

- 462 Ameijeiras, M. P., Godoy, L. A. 2016. Simplified analytical approach to evaluate the nonlinear  
463 dynamics of elastic cylindrical shells under lateral blast loads. *Latin American Journal of*  
464 *Solids and Structures*, 13, 1281-1298. <https://doi.org/10.1590/1679-78252587>
- 465 Antonioni, G., Spadoni, G., Cozzani, V. 2009. Application of domino effect quantitative risk  
466 assessment to an extended industrial area. *Journal of Loss Prevention in the Process*  
467 *Industries*, 22(5), 614-624. <https://doi.org/10.1016/j.jlp.2009.02.012>
- 468 Araki, Y., Hokugo, A., Pinheiro, A. T. K., Ohtsu, N., Cruz, A. M. 2021. Explosion at an aluminum  
469 factory caused by the July 2018 Japan floods: Investigation of damages and evacuation  
470 activities. *Journal of Loss Prevention in the Process Industries*, 69, 104352.  
471 <https://doi.org/10.1016/j.jlp.2020.104352>
- 472 Bedford, T., Cooke, R. 2001. *Probabilistic Risk Analysis: Foundations and Methods*. Cambridge ,  
473 UK : Cambridge University Press.
- 474 Chen, A., Louca, L. A., Elghazouli, A. Y. 2016. Behaviour of cylindrical steel drums under blast  
475 loading conditions. *International Journal of Impact Engineering*, 88, 39-53.  
476 <https://doi.org/10.1016/j.ijimpeng.2015.09.007>
- 477 Choe D., Gardoni P., and Rosowsky D. 2007 Closed-form fragility estimates, parameter sensitivity  
478 and Bayesian updating for RC columns. *Journal of Engineering Mechanics*, 133, 833-843.  
479 [https://doi.org/10.1061/\(ASCE\)0733-9399\(2007\)133:7\(833\)](https://doi.org/10.1061/(ASCE)0733-9399(2007)133:7(833))
- 480 Dadashzadeh, M., Abbassi, R., Khan, F., Hawboldt, K. 2013. Explosion modeling and analysis of  
481 BP deepwater horizon accident. *Safety Science*, 57, 150-160.  
482 <https://doi.org/10.1016/j.ssci.2013.01.024>

Please cite this document as: Stochino, F., Nocera, F., & Gardoni, P. (2022). Physics-based Demand Model and Fragility Functions of Industrial Tanks under blast loading. *Journal of Loss Prevention in the Process Industries*, 77, 104798. DOI: 10.1016/j.jlp.2022.104798

483 Damle, S., Mani, S. K., Balamurugan, G. 2021. Natech guide words: A new approach to assess  
484 and manage Natech risk to ensure business continuity. *Journal of Loss Prevention in the*  
485 *Process Industries*, 104564. <https://doi.org/10.1016/j.jlp.2021.104564>

486 Ding, L., Khan, F., Ji, J. 2022. A novel vulnerability model considering synergistic effect of fire  
487 and overpressure in chemical processing facilities. *Reliability Engineering & System Safety*,  
488 217, 108081. <https://doi.org/10.1016/j.ress.2021.108081>

489 Ditlevsen O. and H. O. Madsen. 1996. *Structural reliability methods*. Wiley, New York.

490 Donnell, L. 1934. A new theory for the buckling of thin cylinders under axial compression and  
491 bending. *Transactions of the ASME*, 56, 795–806.

492 Duong, D. H., Hanus, J. L., Bouazaoui, L., Pennetier, O., Moriceau, J., Prod’homme, G.,  
493 Reimeringer, M. 2012a. Response of a tank under blast loading--part I: experimental  
494 characterisation of blast loading arising from a gas explosion. *European Journal of*  
495 *Environmental and Civil Engineering*, 16(9), 1023-1041.  
496 <https://doi.org/10.1080/19648189.2012.699741>

497 Duong, D. H., Hanus, J. L., Bouazaoui, L., Regal, X., Prod’Homme, G., Noret, E., T. Yalamas ,  
498 Reimeringer, M., Bailly, P., Pennetier, O. 2012b. Response of a tank under blast loading–Part  
499 II: Experimental structural response and simplified analytical approach. *European Journal of*  
500 *Environmental and Civil Engineering*, 16(9), 1042-1057.  
501 <https://doi.org/10.1080/19648189.2012.699743>

502 Freidlander, F.G. 1946 The diffraction of sound pulses. I. Diffraction by a semi-infinite plate.  
503 *Proceedings of the Royal Society A*, 186, 322–344.

Please cite this document as: Stochino, F., Nocera, F., & Gardoni, P. (2022). Physics-based Demand Model and Fragility Functions of Industrial Tanks under blast loading. *Journal of Loss Prevention in the Process Industries*, 77, 104798. DOI: 10.1016/j.jlp.2022.104798

504 Gardoni P., Der Kiureghian A. and Mosalam K.M. 2002 Probabilistic Capacity Models and  
505 Fragility Estimates for Reinforced Concrete Columns based on Experimental Observations.  
506 *Journal of Engineering Mechanics*, 128 1024-1038. [https://doi.org/10.1061/\(ASCE\)0733-](https://doi.org/10.1061/(ASCE)0733-9399(2002)128:10(1024))  
507 [9399\(2002\)128:10\(1024\)](https://doi.org/10.1061/(ASCE)0733-9399(2002)128:10(1024))

508 Gardoni P., Mosalam K.M. and Der Kiureghian A. 2003 Probabilistic seismic demand models and  
509 fragility estimates for RC bridges. *Journal of Earthquake Engineering*, 7 79-106.  
510 <https://doi.org/10.1080/13632460309350474>

511 Gardoni P., Reinschmidt K.F. and Kumar R. 2007 A probabilistic framework for Bayesian  
512 adaptive forecasting of project progress *Computer-Aided Civil and Infrastructure*  
513 *Engineering*, 22 (3), 182-196. <https://doi.org/10.1111/j.1467-8667.2007.00478.x>

514 Gardoni P. and Murphy C. 2014. A scale of risk. *Risk analysis*, 34(7), 1208-1227.  
515 <https://doi.org/10.1111/risa.12150>

516 Gardoni P. 2017 *Risk and Reliability Analysis: Theory and Applications*. Springer International  
517 Publishing.

518 Held, M. 1983 Blast waves in free air. *Propellants, Explosives, Pyrotechnics*, 8, 1–7.

519 HSE. 2009. Buncefield explosion mechanism phase 1 (Technical Report No. RR718). London:  
520 Steel and Construction Institute, Health & Safety Executive.

521 Ibitayo, O. O., Mushkatel, A., Pijawka, K. D. 2004. Social and political amplification of  
522 technological hazards: The case of the PEPCON explosion. *Journal of hazardous materials*,  
523 114(1-3), 15-25. <https://doi.org/10.1016/j.jhazmat.2004.08.020>

Please cite this document as: Stochino, F., Nocera, F., & Gardoni, P. (2022). Physics-based Demand Model and Fragility Functions of Industrial Tanks under blast loading. *Journal of Loss Prevention in the Process Industries*, 77, 104798. DOI: 10.1016/j.jlp.2022.104798

- 524 Hansen, O. R., Hinze, P., Engel, D., Davis, S. 2010. Using computational fluid dynamics for blast  
525 wave predictions. *Journal of Loss Prevention in the Process Industries*, 23, 885-906.  
526 <https://doi.org/10.1016/j.jlp.2010.07.005>
- 527 Huang Q., Gardoni P. and Hurlbaeus S. 2010 Probabilistic seismic demand models and fragility  
528 estimates for reinforced concrete highway bridges with one single-column bent *Journal of*  
529 *Engineering Mechanics*, 136, 1340-1353. [https://doi.org/10.1061/\(ASCE\)EM.1943-](https://doi.org/10.1061/(ASCE)EM.1943-7889.0000186)  
530 7889.0000186
- 531 Iannacone L. and Gardoni P. 2019. Stochastic differential equations for the deterioration processes  
532 of engineering systems. In: *13th International conference on applications of statistics and*  
533 *probability in civil engineering, ICASP*, Seoul, 26–30 May 2019.  
534 <https://doi.org/10.22725/ICASP13.061>
- 535 Jiang, Y., Zhang, B., Wei, J., Wang, W. 2020. Study on the dynamic response of polyurea coated  
536 steel tank subjected to blast loadings. *Journal of Loss Prevention in the Process Industries*,  
537 104234. <https://doi.org/10.1016/j.jlp.2020.104234>
- 538 Lan, M., Gardoni, P., Qin, R., Zhang, X., Zhu, J., Lo, S. 2022. Modeling NaTech-related domino  
539 effects in process clusters: a network-based approach. *Reliability Engineering & System*  
540 *Safety*, 108329. <https://doi.org/10.1016/j.res.2022.108329>
- 541 Landucci, G., Khakzad, N., Reniers, G. 2020. Physical security in the process industry: Theory  
542 with applications, Elsevier.
- 543 Marsh and McLennan, 2016. The 100 Largest Losses 1974-2015. Marsh Ltd.

Please cite this document as: Stochino, F., Nocera, F., & Gardoni, P. (2022). Physics-based Demand Model and Fragility Functions of Industrial Tanks under blast loading. *Journal of Loss Prevention in the Process Industries*, 77, 104798. DOI: 10.1016/j.jlp.2022.104798

- 544 Mayorga, S. Z., Sánchez-Silva, M., Olivar, O. J. R., Giraldo, F. M. 2019. Development of  
545 parametric fragility curves for storage tanks: A Natech approach. *Reliability Engineering &*  
546 *System Safety*, 189, 1-10. <https://doi.org/10.1016/j.ress.2019.04.008>
- 547 Mills, C.A. 1987 The design of concrete structures to resist explosions and weapon effects. *In*  
548 *Proceedings of the 1st International Conference for Hazard Protection*, Edinburgh, Scotland,  
549 27–30 September.
- 550 Misuri, A., Antonioni, G., Cozzani, V. 2020. Quantitative risk assessment of domino effect in  
551 Natech scenarios triggered by lightning. *Journal of Loss Prevention in the Process Industries*,  
552 64, 104095. <https://doi.org/10.1016/j.jlp.2020.104095>
- 553 Murphy C., Gardoni P. and Harris C.E. 2011. Classification and moral evaluation of uncertainties  
554 in engineering modeling. *Science and Engineering Ethics*, 17, 553-570.  
555 <https://doi.org/10.1007/s11948-010-9242-2>
- 556 Nocera F., Tabandeh A., Guidotti R., Boakye J. and Gardoni P. 2019. Physics-based fragility  
557 functions: Their mathematical formulation and use in the reliability and resilience analysis of  
558 transportation infrastructure. in Gardoni P. ed., *Routledge Handbook of Sustainable and*  
559 *Resilient Infrastructure*, Routledge.
- 560 Olmati, P., Petrini, F., Gkoumas, K. 2014. Fragility analysis for the Performance-Based Design of  
561 cladding wall panels subjected to blast load. *Engineering Structures*, 78, 112–120.  
562 <https://doi.org/10.1016/j.engstruct.2014.06.004>
- 563 Ovidi, F., Zhang, L., Landucci, G., Reniers, G. 2021. Agent-based model and simulation of  
564 mitigated domino scenarios in chemical tank farms. *Reliability Engineering & System*  
565 *Safety*, 209, 107476. <https://doi.org/10.1016/j.ress.2021.107476>

Please cite this document as: Stochino, F., Nocera, F., & Gardoni, P. (2022). Physics-based Demand Model and Fragility Functions of Industrial Tanks under blast loading. *Journal of Loss Prevention in the Process Industries*, 77, 104798. DOI: 10.1016/j.jlp.2022.104798

566 PDC-TR 06-08. 2008. *US Army Corps of Engineers, Protective Design Center – Single Degree*  
567 *of Freedom Structural Response Limits for Antiterrorism Design*, USA.

568 Ruiz, C., Salvatorelli-D’Angelo, F., Thompson, V.K. 1989. Elastic response of thin-wall  
569 cylindrical vessels to blast loading. *Computers and Structures*, 32(5), 1061–1072.

570 Salvado, F. C., Tavares, A. J., Teixeira-Dias, F., Cardoso, J. B. 2017. Confined explosions: The  
571 effect of compartment geometry. *Journal of Loss Prevention in the Process Industries*, 48,  
572 126-144.

573 Singh, K., Gardoni, P., Stochino, F. 2020. Probabilistic models for blast parameters and fragility  
574 estimates of steel columns subject to blast loads. *Engineering Structures*, 222, 110944.  
575 <https://doi.org/10.1016/j.engstruct.2020.110944>

576 Sochet, I., Sauvan, P. E., Boulanger, R., Nozeres, F. 2014. External explosion in an industrial site.  
577 *Journal of Loss Prevention in the Process Industries*, 29, 56-64.  
578 <https://doi.org/10.1016/j.jlp.2014.02.001>

579 Stochino, F., Tabandeh, A., Gardoni, P., Sassu, M. 2021. Physics-based probabilistic demand  
580 model and reliability analysis for reinforced concrete beams under blast loads. *Engineering*  
581 *Structures*, 248, 112932. <https://doi.org/10.1016/j.engstruct.2021.112932>

582 Stone, J. C. 1996. A course in probability and statistics, Duxbury, Belmont, California.

583 Suarez-Paba, M. C., Cruz, A. M. 2022. A paradigm shift in Natech risk management: Development  
584 of a rating system framework for evaluating the performance of industry. *Journal of Loss*  
585 *Prevention in the Process Industries*, 74, 104615. <https://doi.org/10.1016/j.jlp.2021.104615>

586 Tabandeh A. and Gardoni P. 2015 Empirical Bayes Approach for developing hierarchical  
587 probabilistic predictive models and its application to the seismic reliability analysis of FRP-

Please cite this document as: Stochino, F., Nocera, F., & Gardoni, P. (2022). Physics-based Demand Model and Fragility Functions of Industrial Tanks under blast loading. *Journal of Loss Prevention in the Process Industries*, 77, 104798. DOI: 10.1016/j.jlp.2022.104798

588 retrofitted RC bridges. *Journal of Risk and Uncertainty in Engineering Systems Part A: Civ.*  
589 *Eng.* 1 04015002. <https://doi.org/10.1061/AJRUA6.0000817>

590 Tabandeh A, Asem P, Gardoni P. 2020 Physics-based probabilistic models: Integrating differential  
591 equations and observational data. *Structural Safety*, 87:101981.  
592 <https://doi.org/10.1016/j.strusafe.2020.101981>

593 Tugnoli, A., Scarponi, G. E., Antonioni, G., Cozzani, V. 2022. Quantitative assessment of domino  
594 effect and escalation scenarios caused by fragment projection. *Reliability Engineering &*  
595 *System Safety*, 217, 108059. <https://doi.org/10.1016/j.res.2021.108059>

596 UFC 3-340-02. *Structures to Resist the Effects of Accidental Explosions*; Department of Defense:  
597 Virginia, VA, USA, 2008.

598 Uijt, D. H. P., Ale, B. J. M. (2005). Guideline for quantitative risk assessment——‘purple book’.

599 Wang Y., Gardoni P., Murphy C. and Guerrier S. 2021. Empirical predictive modeling approach  
600 to quantifying social vulnerability to natural hazards. *Annals of the American Association of*  
601 *Geographers*, 111(5), 1559-1583. <https://doi.org/10.1080/24694452.2020.1823807>

602 Zhong J., Gardoni P. and Rosowsky D. 2009 Bayesian Updating of Seismic Demand Models and  
603 Fragility Estimates for Reinforced Concrete Bridges with Two-Column Bents. *Journal of*  
604 *Earthquake Engineering*, 13, 716-735. <https://doi.org/10.1080/13632460802421334>

605 Zhou, J., Reniers, G. 2020. Probabilistic Petri-net addition enabling decision making depending  
606 on situational change: The case of emergency response to fuel tank farm fire. *Reliability*  
607 *Engineering & System Safety*, 200, 106880. <https://doi.org/10.1016/j.res.2020.106880>

Please cite this document as: Stochino, F., Nocera, F., & Gardoni, P. (2022). Physics-based Demand Model and Fragility Functions of Industrial Tanks under blast loading. *Journal of Loss Prevention in the Process Industries*, 77, 104798. DOI: 10.1016/j.jlp.2022.104798

608 Zio, E., Aven, T. 2013. Industrial disasters: Extreme events, extremely rare. Some reflections on  
609 the treatment of uncertainties in the assessment of the associated risks. *Process Safety and*  
610 *Environmental Protection*, 91(1-2), 31-45. <https://doi.org/10.1016/j.psep.2012.01.004>  
611

Accepted Manuscript

Please cite this document as: Stochino, F., Nocera, F., & Gardoni, P. (2022). Physics-based Demand Model and Fragility Functions of Industrial Tanks under blast loading. *Journal of Loss Prevention in the Process Industries*, 77, 104798. DOI: 10.1016/j.jlp.2022.104798

612 **Nomenclature**

$a$	Vertical abscissa in the cylindrical coordinate system
$B$	Numerical parameter equal to $E_s e^3 / (12(1 - \nu^2))$ ,
$C(\mathbf{x})$	Capacity model associated the performance thresholds
$D(\mathbf{x}, \Theta)$	Demand model
$d$	Tank diameter
$E_s$	Steel elastic modulus
$e$	Tank thickness
$F_A(s, \omega, a)$	Airy stress function
$F(\mathbf{s}, \Theta)$	Fragility function
$\hat{F}(\mathbf{s})$	Point-estimate of the fragility
$\tilde{F}(\mathbf{s})$	Predictive estimate of the fragility
$f_{dyn}$	Steel dynamic yielding strength
$f_{stat}$	Steel static yielding strength
$f(\Theta)$	posterior PDF of $\Theta$
$h$	Tank height [m]
$h_{k,j}(\mathbf{x})$	Explanatory functions
$g(\mathbf{x}, \Theta)$	Limit-state function
$I_{SO}$	Incident impulse
$K$	Equivalent stiffness
$L(\Theta)$	Likelihood function that captures the information on $\Theta$

Please cite this document as: Stochino, F., Nocera, F., & Gardoni, P. (2022). Physics-based Demand Model and Fragility Functions of Industrial Tanks under blast loading. *Journal of Loss Prevention in the Process Industries*, 77, 104798. DOI: 10.1016/j.jlp.2022.104798

$M$	Equivalent load
$N_s$	Distributed axial stress
$N_{s\omega}$	Distributed shear stress
$N_\omega$	Distributed circumferential stress
$P_{ref}$	Reflected peak pressure [kPa]
$P_{atm}$	Atmospheric pressure
$P_{so}$	Stand-off pressure
$p(\Theta)$	Prior distribution reflecting our state of knowledge about $\Theta$
$Q_n$	Numerical parameter equal to $(16Dn^4/d^4 + E\pi^4d^2/(4n^4H^4))/(\rho e)$
$q$	Blast load pressure
$\mathbf{R}$	Correlation matrix
$R$	Stand-off distance
$r_{ki}(\Theta_k)$	Residual of the prediction for the $i^{th}$ datum
$r_t$	Tank radius
$s$	Radial abscissa in the cylindrical coordinate system
$t$	Time
$t_d$	Positive phase duration
$T_k(\cdot)$	Transformation function
$Y_k(\mathbf{x}, \Theta_k)$	$k^{th}$ quantity of interest
$\hat{y}_k(\mathbf{x})$	Existing deterministic model to predict $Y_k$
$u$	Axial displacement

Please cite this document as: Stochino, F., Nocera, F., & Gardoni, P. (2022). Physics-based Demand Model and Fragility Functions of Industrial Tanks under blast loading. Journal of Loss Prevention in the Process Industries, 77, 104798. DOI: 10.1016/j.jlp.2022.104798

$v$	Circumferential displacement
$W$	Mass of explosive in kg of equivalent TNT
$w$	Radial displacement
$\mathbf{x}$	Vector of basic variables that characterize $Y_k$
$z$	Scaled distance
$\alpha$	Bending rotation
$\beta(\mathbf{s}, \boldsymbol{\Theta})$	Reliability index
$\gamma_k(\mathbf{x}, \boldsymbol{\theta}_k)$	Correction term constructed to improve the prediction of $\hat{y}_k(\mathbf{x})$
$\varepsilon_k$	Standard normal random variable
$\boldsymbol{\theta}$	Vector of model parameters
$\boldsymbol{\Theta}_k = (\boldsymbol{\theta}_k, \sigma_k)$	Vector of unknown model parameters
$\kappa$	Normalizing constant.
$\lambda$	Parameter equal to $2nh/\pi d$
$\mu_{\theta_{k,i}}$	Posterior mean of $\theta_{k,i}$
$\nu$	Poisson coefficient
$\rho$	Specific mass
$\boldsymbol{\Sigma}$	Covariance matrix
$\sigma_k$	Standard deviation of the model error
$\sigma_{\theta_{k,i}}$	Standard deviation of $\theta_{k,i}$ .
$\Phi(\cdot)$	Standard Normal cumulative density function
$\varphi(\cdot)$	Standard Normal probability density function
$\Omega_n$	Numerical parameter equal to $(16Dn^4/(d^4) + Ee\pi^4 d^2/(4n^4 H^4))/(\frac{2n^2}{d})$

Please cite this document as: Stochino, F., Nocera, F., & Gardoni, P. (2022). Physics-based Demand Model and Fragility Functions of Industrial Tanks under blast loading. Journal of Loss Prevention in the Process Industries, 77, 104798. DOI: 10.1016/j.jlp.2022.104798

$\omega$	Angular coordinate in the cylindrical coordinate system
$\omega_c$	Angular distance between maximum and minimum deflection

613

Accepted Manuscript

Please cite this document as: Stochino, F., Nocera, F., & Gardoni, P. (2022). Physics-based Demand Model and Fragility Functions of Industrial Tanks under blast loading. *Journal of Loss Prevention in the Process Industries*, 77, 104798. DOI: 10.1016/j.jlp.2022.104798

614 **Appendix**

615 Table A1. Values of  $z$  for each tank in the first scenario

Tank	$z$
1	8.20
2	4.20
3	4.61
4	7.23
5	4.89
6	2.69

616

617 Table A2. Values of  $z$  for each tank in the second scenario

Tank	$z$
1	6.66
2	5.57
3	6.61
4	3.78
5	1.61
6	3.71

618

Please cite this document as: Stochino, F., Nocera, F., & Gardoni, P. (2022). Physics-based Demand Model and Fragility Functions of Industrial Tanks under blast loading. *Journal of Loss Prevention in the Process Industries*, 77, 104798. DOI: 10.1016/j.jlp.2022.104798

619

620 Table A3. Values of  $z$  for each tank in the third scenario

Tank	$z$
1	2.26
2	5.40
3	8.56
4	3.40
5	6.02
6	8.97

621

Accepted Manuscript

Please cite this document as: Stochino, F., Nocera, F., & Gardoni, P. (2022). Physics-based Demand Model and Fragility Functions of Industrial Tanks under blast loading. *Journal of Loss Prevention in the Process Industries*, 77, 104798. DOI: 10.1016/j.jlp.2022.104798